



23 ***ABSTRACT***

24

25 Advances in sequencing technologies have facilitated the genetic characterization of large numbers of  
26 clinical cancer samples, leading to accumulation of extensive amounts of data. While potentially very  
27 useful for directing research and for clinical decision making, the increasing quantity of data generates  
28 challenges in its optimal management, and translation to informing clinical and research questions.  
29 Here, we present Database Of Recurrent Mutations (DORM), a database listing recurrent mutations  
30 (tissue-agnostic population frequency > 1) identified from cancer samples analyzed with whole genome  
31 or whole exome sequencing. The DORM database is a fast and feature-rich database supporting  
32 searching for several proteins, amino acid substitutions as well as queries using regular expressions.

## 33 ***INTRODUCTION***

34

35 The fast-paced development of next-generation sequencing (NGS) technology and its use to  
36 study cancer specimens has led to an accumulation of large amounts of data and establishment  
37 of expansive databases that have propelled the discovery of predictive and therapeutic  
38 biomarkers for various cancers (Campbell *et al.* 2020). Large-scale sequencing efforts have  
39 pinned somatic mutations as the most common cause of human cancers (Martincorena and  
40 Campbell 2015). Mutations in several oncogenes are well-characterized driver events in  
41 various cancers, e.g. mutations in KRAS G12 residue in pancreatic and lung cancer (Hong *et*  
42 *al.* 2020), BRAF V600 in melanoma (Hauschild *et al.* 2012), and the EGFR L858 in lung  
43 cancer (Lynch *et al.* 2004; Paez *et al.* 2004). Despite their frequent observations in the clinic,  
44 these hotspot mutations actually make up a small proportion of all the cancer-associated  
45 mutations and there are a large number of recurrent, but “non-hotspot” mutations (Chang *et al.*  
46 2016).

47 Databases presenting cancer-associated mutations like COSMIC  
48 (<https://cancer.sanger.ac.uk>) (Tate *et al.* 2019), the ICGC data portal (<https://dcc.icgc.org>)  
49 (Zhang *et al.* 2011), AACR GENIE (<https://genie.cbioportal.org>) (The AACR Project GENIE  
50 Consortium 2017), and cBioportal (<https://www.cbioportal.org/>) (Cerami *et al.* 2012; Gao *et*  
51 *al.* 2013) present a well-designed interface that provides access to rich data. However, by  
52 design, these databases with comprehensive information use a significant amount of bandwidth  
53 as well as require multiple steps to access to key pieces of information, like the frequency of  
54 mutations and the affected amino acid residues. Especially, calculation of the latter requiring  
55 manual processing of the data, as there is no direct way to retrieve this information from any  
56 of these large databases.

57           We sought to solve these shortcomings and built a database of recurrent mutations using  
58 the large COSMIC cancer registry as a model. Our goal with this project was to develop and  
59 deploy a fast and lightweight web-tool to give the user a quick-and-easy way to check the status  
60 of a particular mutation of interest in cancer samples in an easy-to-understand format. In  
61 addition to direct time-savings, we believe initiatives like ours, help further cancer research  
62 and its global outreach by improving accessibility to well-summarized information. Moreover,  
63 we hope that our open-source framework enables applications to other public cancer registries  
64 and diversification to other frontiers of healthcare.

## 65 ***MATERIALS AND METHODS***

66

### 67 **Website and web server**

68 The DORM database is accessible at <https://eleniuslabtools.utu.fi/tools/DORM/Mutations/>,  
69 and all requests to the server are handled by an NGINX reverse-proxy (<https://nginx.org/>) that  
70 encrypts the traffic between our server and the end-user's web-browser. The connection is  
71 encrypted using the latest Transport Layer Security (TLS) cryptographic protocol 1.3 (Rescorla  
72 2018) and an industry standard 256-bit Advanced Encryption Standard (AES-256) (National  
73 Institute of Standards and Technology 2001). Additionally, as a fallback, the server of DORM  
74 also supports connections over TLS 1.2 to support legacy hardware and browsers. The landing  
75 page website and the documentation is built using HTML5, CSS and JavaScript. The web tools  
76 are built using Shiny (Chang *et al.* 2021) and R (R Core Team 2018). These services are hosted  
77 on a virtual private server at the premises of University of Turku, Turku, Finland. The source  
78 code for deploying DORM as an R Shiny app is available at  
79 [https://github.com/dchakro/DORM\\_Mutations](https://github.com/dchakro/DORM_Mutations) repository.

80

### 81 **Hardware**

82 *Database processing & analysis:* Apple iMac (early 2013) equipped with Intel Core i5 CPU (4  
83 cores – 3.2 GHz), 24 GB DDR3 RAM, 500 GB SSD running macOS Catalina 10.15.

84 *Server:* Virtual private server (KVM virtualization) with Intel(R) Xeon(R) Gold 5120 CPU (1  
85 core – 2.20 GHz), 6 GB ECC RAM, 100 GB HDD running Ubuntu 18.04 LTS.

86 *Web performance testing:* Apple MacBook Pro (early 2015) equipped with an Intel Core i5  
87 CPU (2 cores – 2.7 GHz), 8 GB DDR3 RAM, 500 GB SSD running macOS Catalina 10.15.

88 The device was connected via a 5 GHz Wi-Fi router to the public ISP (i.e., outside the network  
89 where the DORM database is hosted) over a 100 Mbps fiber optic broadband connection.

90

## 91 **Data and processing of data**

92 Data were acquired from COSMIC release v95 (released November 24, 2021  
93 <https://cancer.sanger.ac.uk>) as a GNU zip (GZIP) archive of the tab-delimited text file with all  
94 mutations identified from genome-wide screens (includes data from whole genome  
95 sequencing, and whole exome sequencing). The samples from targeted screens were excluded  
96 to ensure our analysis is free from selection bias and so that, for a particular tissue, the  
97 frequency of mutations between different proteins can be compared directly.

98 *Pre-processing:* The decompressed data (16.03 GB) is processed using the "awk" programming  
99 language (Aho, Kernighan and Weinberger 1988) to select relevant columns (named, Gene  
100 name, Sample name, Primary site, Primary histology, Genome-wide screen, Mutation CDS,  
101 Mutation AA). This step reduces the size of the data matrix by  $\approx 80\%$ , thereby, decreasing the  
102 computation time and computational resource requirements for the downstream analyses. The  
103 selected columns were read in R by using the `data.table::fread()` function (Dowle and  
104 Srinivasan 2021). The complete database was stored as standard R object in the .RDS file  
105 format, with a notable difference: instead of `saveRDS` from R “base”, which uses serialized  
106 compression, parallelized GZIP (pigz: <https://zlib.net/pigz/>) was used for compression –  
107 decompression. This enabled usage of multiple CPU threads to speed up the read-write  
108 operations, and in our case was limited by disk I/O. The functions for reading-writing R objects  
109 in .RDS files using parallelized compression-decompression are [described in this R script](#).

110 *Filtering:* The duplicate entries for mutations attributed to ENSEMBL transcripts ( $n = 30.8 \times$   
111  $10^6$ ) were removed (**Supplementary Figure S1**). Mutations with unknown consequences on the  
112 protein level ( $n = 8.8 \times 10^6$ ) were removed, leaving  $6.4 \times 10^6$  coding alterations. From these,  
113 silent mutations ( $n = 1.5 \times 10^6$ ) i.e., nucleotide substitutions leading to no changes at the amino  
114 acid level (this phenomenon happens due to codon degeneracy (Watson *et al.* 2007)) were

115 removed (**Supplementary Figure S1**). To retain only unique entries, a mutation ID was created  
116 using the sample name, protein name and the amino acid change. Samples with duplicate  
117 mutation IDs ( $n = 78,569$ ) were removed (**Supplementary Figure S1**). The filtered database  
118 with unique coding mutations ( $n = 4.8 \times 10^6$ ) were stored as a parallelized GZIP .RDS file,  
119 enabling faster load times. Searching and parsing of the text was done using the ‘stringi’ R  
120 package (Gagolewski 2021).

121 *Processing:* Mutations with single occurrences (i.e., frequency = 1) were removed ( $n = 2.9 \times$   
122  $10^6$ ) from the list of unique coding mutations, as they are not part of the pool of recurrent  
123 mutations. For each mutation, its cumulative frequency of occurrence, as well as its frequency  
124 in cancers of various tissues, was calculated and compiled into a table. The table was sorted by  
125 mutation frequency (total number of samples across all cancers) and then stored as a  
126 parallelized-GZIP .RDS file.

127 *Updates:* Since 2004, marking the release of COSMIC v1, the dataset has been updated on  
128 average four times per year (range: 11 releases in 2006 and two releases in 2020). The COSMIC  
129 data releases need to be acquired from (<https://cancer.sanger.ac.uk>), then our optimized  
130 pipeline can be run with a shell script that automates the processing and generation of the  
131 underlying database for DORM.

132

### 133 **Benchmarking and testing performance**

134 To evaluate the performance of different code blocks, the ‘microbenchmark’ R package  
135 (Mersmann 2021) was used to gather data. The data were graphically represented using  
136 Graphpad Prism 9. Statistical testing comparing multiple groups was performed using Brown  
137 Forsythe and Welch ANOVA test and correction for multiple testing was done by controlling  
138 the false discovery rate using the two-stage step-up method of Benjamini, Krieger and

139 Yekutieli (Benjamini, Krieger and Yekutieli 2006) in Graphpad Prism 9. Statistical testing  
140 comparing two groups of observations was done using Welch's t-test in Graphpad Prism 9. The  
141 code blocks used for testing and benchmarking their performance is available at  
142 <https://github.com/KE-group/DORM-2022> repository.

143 The performance of the websites hosting the databases was measured on Google  
144 Chrome (v. 97.0.4692.99) with Google Lighthouse (v. 8.5.0) (available in Chrome DevTools).  
145 Lighthouse (<https://github.com/GoogleChrome/lighthouse>) is an open-source tool for  
146 automated auditing and assessing performance metrics. A search for EGFR mutations was done  
147 on the five databases (DORM, COSMIC, ICGC, cBioPortal and AACR GENIE), and links  
148 (**Supplementary Table 1**) to those individual searches were used to test the performance of the  
149 databases. This was done to discount the varying duration required to do the same search on  
150 the four databases. Lighthouse 8 produces a performance score which is a weighted average of  
151 First Contentful Paint (10%, marks the time at which the first text or image is painted), Speed  
152 Index (10%, shows how quickly the contents of a page are visibly populated), Largest  
153 Contentful Paint (25%, marks the time at which the largest text or image is painted), Time to  
154 interactive (10%, the amount of time it takes for the page to become fully interactive), Total  
155 Blocking Time (30%, measures the total amount of time that a page is blocked from responding  
156 to user input), and Cumulative Layout Shift (15%, measures the unexpected movement of page  
157 content). The JSON data in the lighthouse reports was parsed using the 'jsonlite' R package  
158 (Ooms 2014) and tabulated in R. The data were graphically represented using Graphpad Prism  
159 9. Statistical testing comparing multiple groups was performed either using Brown Forsythe  
160 and Welch ANOVA test or Kruskal-Wallis test. Correction for multiple testing was done by  
161 controlling the false discovery rate using the two-stage step-up method of Benjamini, Krieger  
162 and Yekutieli (Benjamini, Krieger and Yekutieli 2006) in Graphpad Prism 9.

163



## 164 **RESULTS**

165

### 166 **Optimizing R code for speed and efficiency**

167 In order to maximize the efficiency throughout our pipeline, we benchmarked common  
168 workflows that can be used to resolve the computation bottlenecks. There are several packages  
169 for reading data into R, and we discovered that `data.table::fread()` function offered the  
170 best performance in reading both small and big (tested with  $10^5$  rows) tables. In our tests,  
171 `data.table::fread()` was faster ( $q < 0.0001$ ) than `base::read.table()` in reading  
172 files containing  $10^3$  and  $10^5$  rows (**Supplementary Figure S2 A-B**). As intended by the  
173 developers of the ‘readr’ and ‘vroom’ package, their individual functions for reading TSV files  
174 were faster than `fread` for large files ( $q < 0.001$ ), but, they were slower by a factor of 16-20 for  
175 smaller files ( $q < 0.0001$ ) (**Supplementary Figure S2 A-B**). Furthermore, the `data.table`  
176 implementation of generating a frequency table was more efficient ( $q < 0.0001$ ) than  
177 alternatives like `base::table()` and `plyr::count()` (**Supplementary Figure S2 C**).  
178 Consequently, we used `data.table` as the background framework for reading and managing  
179 tabular data throughout our analysis pipeline, as well as in the backend of the R Shiny web tool  
180 for DORM.

181 Filtering a large database requires extensive use of search, and the search-replace  
182 functionality is required for parsing and cleaning up data fields. We found that alternatives  
183 from ‘stringi’ were faster than their counterparts in R base ( $P < 0.0001$ ) (**Supplementary Figure**  
184 **S2 D**) in carrying out these operations. Furthermore, in comparison to `base::grep()`, we  
185 observed considerable improvements in speed (500-fold reduction,  $q < 0.0001$ ) by using GNU-  
186 grep for searching the data (stored on disk) server-side when a query was received by the R  
187 Shiny web tool (**Supplementary Figure S2 E**). Therefore, the fastest approach to process the  
188 search queries (entered by a user in the interface), was to execute the search using GNU-grep

189 on the DORM database (stored in plain text) and read the output in R. This intermediate file  
190 containing the search results is deleted after being read in R (to plot and display the results on  
191 the user's browser) to uphold the user's privacy.

192 With large datasets, parallel computation, is known to improve performance (Nagurney  
193 1996). Indeed, even with our limited four CPU-core (x86-64 architecture) setup, we observed  
194 performance improvements by using a parallelized version of the code. The gathered data  
195 indicated that parallelizing appropriate repetitive tasks with constructs such as  
196 `foreach::foreach()` and `parallel::mclapply()`, offer significant reductions in  
197 processing time (**Supplementary Figure S2 F**). The `mclapply()` implementations were the  
198 fastest methods across our range of tested number of operations (range: 600 – 60000)  
199 (**Supplementary Figure S2 F**). It is noteworthy that, in case of the `foreach` package, the gains in  
200 performance were dependent on the size of data, i.e., with smaller loops (600 operations) set  
201 significant overheads were incurred while setting up an environment for parallel processing  
202 (**Supplementary Figure S2 F**). Additionally, similar improvements were observed by  
203 paralling the operations of saving and loading the standard `.RDS` file format in comparison  
204 to `base::saveRDS()` and `base::readRDS()` methods (**Supplementary Figure S2 G-H**).

205

## 206 **Contemporary databases are slow and resource intensive**

207 One of the primary goals of DORM was to display the desired statistics and results faster than  
208 the contemporary databases like COSMIC, the ICGC data portal, cBioPortal and AACR  
209 GENIE data portal. To this end, Google Lighthouse was used to benchmark the performance  
210 of these databases and compare it to that of DORM to understand an end-user's experience.  
211 DORM scored better than all the four databases (mean score for DORM: 84.7, COSMIC: 43.2,  
212 ICGC: 24.5, cBioPortal: 21, GENIE: 20.83) (**Figure 1 A**). In addition to taking the lowest time  
213 to become fully interactive (**Figure 1 B**), DORM was the only database that had zero seconds

214 of blocking time (i.e., DORM remained responsive to user input) (**Figure 1 C**). Regarding  
215 client-side memory management, DORM had the lowest peak RAM usage (**Figure 1 D**), and  
216 the lowest RAM usage after garbage collection (i.e., after the browser was left to idle for 2  
217 minutes) (**Supplementary Figure S3 A**) among the tested databases. Lighthouse performance  
218 score is a weighted mean of six individual parameters, namely, First Contentful Paint, Speed  
219 Index, Largest Contentful Paint, Time to interactive, Total Blocking Time, Cumulative Layout  
220 Shift, (details described in the materials & methods section titled “Benchmarking and testing  
221 performance”). The individual observations are plotted in **Figure 1 B-C** and **Supplementary**  
222 **Figure S3 B-E**.

223

#### 224 **Identifying recurrent coding mutations after eradicating duplicate entries**

225 All the major cancer databases (like COSMIC, cBioPortal, GENIE) which source information  
226 from multiple institutions share the common problem of mutations being reported multiple  
227 times due to same samples being included in different publications and/or studies. To counter  
228 this rampant issue of duplicate entries, we devised a mutation ID by using a combination of  
229 sample name, the protein name and the amino acid change and used it to remove the entries  
230 with duplicate mutation IDs. From the list of genuine coding mutations, COSMIC v95 had  
231 78,569 duplicates, constituting 1.60 % of the filtered coding mutations (**Supplementary Figure**  
232 **S1**). After filtering out the non-recurrent mutations (i.e., mutations with a tissue-agnostic  
233 population frequency of 1), the data consists of 1,887,757 recurrent mutations which are  
234 comprised of 673,033 individual mutations (**Supplementary Figure S1**).

235 Interestingly, some samples ( $n = 1,207$ ) in the dataset exclusively harbor non-recurrent  
236 coding mutations (**Supplementary Figure S4 A**), and overall, these individual samples belong  
237 to cancers of hematopoietic and lymphoid tissues, kidney, and autonomic ganglia  
238 (**Supplementary Figure S4 A**) and have very few coding mutations (range: 1 to 43 mutations

239 per sample) (**Supplementary Figure S4 B**). On average, out of the total number of mutations  
240 across the 39 tissues included in the analysis, 39.1% of the mutations were recurrent (i.e.,  
241 tissue-agnostic population frequency  $>1$ ) in nature (**Supplementary Figure S4 C**). The highest  
242 percentage of recurrent mutations could be found in penile cancers (92.6%,  $n = 1,195$   
243 mutations; sample size = 10), thyroid cancers (89.6%;  $n = 139,883$  mutations; sample size =  
244 989) and meningeal malignancies (56.1%;  $n = 2,401$  mutations; sample size = 163)  
245 (**Supplementary Figure S4 C**). The largest number of non-recurrent mutations were in cancers  
246 of the skin, large intestine, and lungs and together these contribute 48.5% of all the non-  
247 recurrent mutations. However, this was expected, as the samples from these three tissues also  
248 contribute a total of 46.6% of all the coding mutations in the dataset (**Supplementary Figure S4**  
249 **C**).

250 The median mutational load (defined as the number of mutations per sample) in the  
251 dataset was 42 mutations/sample (mean ( $\mu$ ): 141, IQR: 81), with several outliers in different  
252 cancer types (**Supplementary Figure S4 D**). On average, samples from cancers of the  
253 endometrium ( $\mu = 564$ ), skin ( $\mu = 508$ ), and placenta ( $\mu = 393$ ) had the highest mutation load  
254 while samples from the autonomic ganglia ( $\mu = 16$ ), eye ( $\mu = 16.8$ ) and the adrenal gland ( $\mu =$   
255 19) had the lowest (**Supplementary Figure S4 D**).

256

### 257 **Top recurrent mutations**

258 Among the 100 most-recurrent mutations, the highest number of mutations are reported in  
259 TP53 (number of variants [ $n$ ] = 19, frequency in cohort [ $v$ ] = 3,779), followed by KRAS ( $n =$   
260 9,  $v = 3,006$ ), PIK3CA ( $n = 6$ ,  $v = 1,808$ ), BRAF ( $n=1$ ,  $v = 1,432$ ), and NRAS ( $n=5$ ,  $v = 773$ )  
261 (**Figure 2**). Among these 100 recurrent mutations, 19 mutations ( $v = 9,438$ ) were in oncogenes,  
262 and 11 mutations ( $v = 5,349$ ) in tumor suppressor genes. The top three recurrent mutations

263 were the amino acid substitutions BRAF V600E ( $v = 1,432$ ), KRAS G12D ( $v = 977$ ) and KRAS  
264 G12V ( $v = 784$ ) (Figure 2).

265 The survey of the cancer genomes, conducted here, was free from the selection bias that  
266 is introduced with targeted panels and selected sequencing. Although, while those are cost-  
267 effective strategies to identify driver and predictive mutations for cancers of selected  
268 histologies, they cause an over-representation of genes (and mutations in those genes) that are  
269 included in the selected panels which masks the true frequency of mutations in tumor tissues.  
270 This disparity was evident by the fact that EGFR L858R, the hotspot driver mutation in lung  
271 adenocarcinoma, ranked 84<sup>th</sup> ( $v = 75$ ) in the list of most frequent amino acid substitutions  
272 (Figure 2). By contrast, it ranks 6<sup>th</sup> ( $v = 10,631$ ) when data from the targeted screens are also  
273 incorporated in computation of population frequencies.

274

### 275 **Website to browse the recurrent mutations**

276 The processed database is hosted on a web server at the University of Turku and can be  
277 accessed at the URL <https://eleniuslabtools.utu.fi/tools/DORM/Mutations> (Figure 3). On  
278 receiving a connection request, the Shiny (<https://shiny.rstudio.com/>) web server spawns a new  
279 instance and displays the 50 mutations with the highest rate of recurrence. At the top of a page,  
280 there is a plot panel that consists of two dynamic plots that are updated in real-time in response  
281 to the user's search queries. The bar plot on the left shows the cumulative frequency of the  
282 individual recurrent mutations in the population (Figure 3 A). The bar plot on the right shows  
283 the 25-most frequently mutated proteins across all the samples for the selected tissue (Figure 3  
284 B). The plot is rendered as a high-resolution image in the user's web browser in accordance  
285 with the browser's dimensions and can be saved as an image straight from the browser. Query  
286 term(s) can be entered in the search bar (Figure 3 C), which updates the results in the table  
287 (Figure 3 D) showing the protein, the mutation, the aggregate frequency in the population, and

288 the frequencies categorized by the primary site of the cancer. The results displayed in the table  
289 can be readily copied to a spreadsheet. Next to the search bar, there is a dropdown menu (**Figure**  
290 **3 E**) to limit the number of results displayed in the table and the plot. The search or browsing  
291 can be restricted to a particular tissue from the menu (**Figure 3 F**). In addition to a button to  
292 reset the website and various parameters to their default value (**Figure 3 G**), there is a button to  
293 generate a direct link to a particular search (**Figure 3 H**). Clicking this button opens a dialog  
294 box (shown in **Figure 3 I**), with the link that can be used to perform the same search with the  
295 exact selected parameters. Clicking this button saves the search term(s) and the set parameter(s)  
296 anonymously on our server (i.e., no identifiable information is stored). Links like these  
297 facilitate sharing of the results, in addition to making it easy to repeat a search without having  
298 to enter the terms and set the parameters manually.

299

### 300 **Searching the database**

301 The user can search the database with terms such as “KRAS” (protein symbol), “V600E” (exact  
302 mutation), or “L858” (amino acid residue). The functions implemented in R and Shiny for  
303 searching the data were slow and unable to process a multi-term search query like “KRAS  
304 G12”. To facilitate this, a custom search function was written where a multi-term search query  
305 gets decomposed into constituent terms and the database is searched with GNU-grep  
306 (<https://www.gnu.org/software/grep/>) in a hierarchical manner. For instance, the server  
307 processes the above-mentioned search query by first shortlisting all the mutations in KRAS,  
308 then selecting only the mutations at the residue Gly 12. The search results are subsequently  
309 read and processed in R. Simultaneously, the plot panels are redrawn to correspond to these  
310 results and the user’s browser is updated with the search results. Depending on the search  
311 complexity and the number of results to be displayed, all of this computation happens within

312 fractions of a second and the results are transmitted securely (TLS encryption) to the user's  
313 web browser.

314 Circumstantially, when the search results consist of just a single protein (like “KRAS  
315 G12” mentioned above), the plot in the right panel changes to a bar plot showing the  
316 distribution of the tissues harboring the specific mutation(s) (Figure 4 A) that are displayed in  
317 the table. On the other hand, when a search result contains several proteins, the plot in the right  
318 panel changes to a pie showing the distribution of mutations in those proteins (Figure 4 B).

319

### 320 **Advanced search using regular expressions**

321 The search bar (shown in Figure 3 C) in the DORM database supports advanced search using  
322 regular expressions. Regular expressions are an important tool in computational and data  
323 science and have been around since their inception in the 1950s (Kleene 1956). Regular  
324 expressions are a sequence of characters that define a set of strings and are a core component  
325 of almost all modern programming languages. In bioinformatics, regular expressions have been  
326 used in a myriad of diverse applications like establishing databases (Bairoch, Bucher and  
327 Hofmann 1997), determination of motifs from aligned protein sequences (Huang 2001), and in  
328 performing multiple sequence alignments (Arslan 2005). The language of regular expressions  
329 is known to have several dialects (i.e., syntax) (Zheng *et al.* 2021), and DORM supports the  
330 UNIX POSIX style regular expressions (IEEE and The Open Group 2018). A brief description  
331 and examples are presented here:

332 1) The pipe, i.e., | symbol, can be used for *either-or clause*, e.g., ‘ERBB | EGFR’ lists  
333 mutations in proteins EGFR, ERBB2, ERBB3 and ERBB4.

334 2) The square brackets, i.e., [ ABC ] structure, can be used to specify inclusions, e.g.,  
335 ‘NRG[ 1–4 ]’ matches only the four of the Neuregulin ligands (NRG1, NRG2, NRG3,  
336 and NRG4). On the other hand, if we want to exclude results that can be done with

337 [ ^abc ] construct, e.g., ‘ERBB[ ^4 ]’ only matches ERBB2 and ERBB3 among the  
338 ERBB proteins leaving out ERBB4.

339 3) Word boundaries can be set with \< and \> operators, e.g., ‘RAS\>’ matches all  
340 the proteins ending in ‘RAS’.

341 4) Match length modifying operators like \*, ?, +, and {m,n} are used to specify zero or  
342 more, at most one, at least one, or repetition for at least m times and at most n times  
343 respectively.

344 With the help of these regular expression operators one can formulate complex queries;  
345 for instance, if we are interested in searching the entire EGFR family of proteins (Yarden 2001)  
346 with one query, we can use a specific query like this:

347 ‘ERBB[234] | [HB]{0,1}EGF[R]{0,1}\> | NRG[1-4] | \<EP[GR]\> | AREG | BTC | TGFA’

348 In the human protein repertoire, this regular expression matches the four receptors from  
349 the ERBB-family EGFR, ERBB2, ERBB3, ERBB4, and their eleven ligands AREG, BTC,  
350 TGFA, NRG1, NRG2, NRG3, NRG4, EGF, HBEGF, EPG and EGR; and nothing more (Figure  
351 4 C).

352



353 ***DISCUSSION***

354

355 Next-generation sequencing (NGS) of cancer sample series has enabled more accurate  
356 understanding of cancer biology and helped to identify new predictive and therapeutic  
357 biomarkers. Here, we present DORM, a fast ([Figure 1 and Supplementary Figure S3](#)) and  
358 feature-rich ([Table 1](#)) web tool, which allows browsing its database that is derived from an  
359 unbiased analysis of somatic mutations identified by whole genome or whole exome NGS  
360 (consists of 91% of the coding mutations present in the COSMIC v95 data release). This  
361 strategy avoids encounters with the ill-effects of the selection biases that are introduced with  
362 the use of targeted NGS panels.

363 In addition to be performant and fast ([Figure 1 and Supplementary Figure S3](#)), DORM has  
364 several advantages ([Table 1](#)), most notably the ability to directly search for sets of proteins and  
365 use regular expressions. Additionally, DORM is the only database that can summarize the  
366 mutations at an amino acid residue level, (this feature is accessible by clicking “DORM-  
367 Residues” link at the top of the page) (direct link:  
368 <https://eleniuslabtools.utu.fi/tools/DORM/Residues/>). Data from all other databases requires  
369 manual processing to retrieve this information. DORM is also the only database to allow the  
370 user to view a large amount of the data without having to click through numerous pages of  
371 results (on DORM, users can choose from a range of 10-10000 results to display). DORM is  
372 also the only database that is free of cookies, trackers, and any embedded analytics.

373 COSMIC, cBioPortal and AACR Genie feature duplicate entries, while DORM and  
374 ICGC do not. Individual mutations, like KRAS G12C, can be directly searched on DORM as  
375 well as COSMIC. The cBioPortal, and the AACR GENIE (based on the cBioPortal user  
376 interface) do not offer the users to limit the search to specific tissues. On ICGC the

377 implementation is similar to DORM (i.e., requires selection from a menu), but on COSMIC the  
378 user has to click the tissue from a table in the “Tissue distribution” section.

379 In the quest for speed and performance, certain compromises had to be made that  
380 constitute the limitations of DORM (Table 2). For instance, DORM does not incorporate or  
381 display the information about copy number variations or structural variations and has stripped  
382 all the detailed sample- and study-level information. Like some other databases in our  
383 comparison, DORM also doesn’t display fusions or non-coding mutations, allow selecting  
384 multiple tissues, and display a lollipop diagram which are a nice tool that place the mutations  
385 in context of the primary sequence of the proteins.

386 DORM is lightweight, and, by using our open-source codebase (see methods for links  
387 to the repositories), it can be run on normal consumer hardware. DORM is publicly available  
388 on a virtual private server that allows us to scale up the resources with an increase in demand.  
389 We believe that DORM can improve accessibility of the important information about recurrent  
390 mutations by being faster and by consuming lesser resources than the competition.

391 **REFERENCES**

- 392 Aho AV, Kernighan BW, Weinberger PJ. *The AWK Programming Language*. Addison-Wesley  
393 Publishing Company, 1988.
- 394 Arslan AN. Multiple Sequence Alignment Containing a Sequence of Regular Expressions. *2005 IEEE*  
395 *Symposium on Computational Intelligence in Bioinformatics and Computational Biology*. La  
396 Jolla, CA, USA: IEEE, 2005, 1–7.
- 397 Bairoch A, Bucher P, Hofmann K. The PROSITE database, its status in 1997. *Nucleic Acids Res*  
398 1997;**25**:217–21.
- 399 Benjamini Y, Krieger AM, Yekutieli D. Adaptive linear step-up procedures that control the false  
400 discovery rate. *Biometrika* 2006;**93**:491–507.
- 401 Campbell PJ, Getz G, Korbelt JO *et al.* Pan-cancer analysis of whole genomes. *Nature* 2020;**578**:82–93.
- 402 Cerami E, Gao J, Dogrusoz U *et al.* The cBio Cancer Genomics Portal: An Open Platform for Exploring  
403 Multidimensional Cancer Genomics Data. *Cancer Discov* 2012;**2**:401–4.
- 404 Chang MT, Asthana S, Gao SP *et al.* Identifying recurrent mutations in cancer reveals widespread  
405 lineage diversity and mutational specificity. *Nat Biotechnol* 2016;**34**:1–11.
- 406 Chang W, Cheng J, Allaire JJ *et al.* *Shiny: Web Application Framework for R.*, 2021.
- 407 Dowle M, Srinivasan A. *Data.Table: Extension of `data.Frame`.*, 2021.
- 408 Gagolewski M. stringi: Fast and portable character string processing in R. *J Stat Softw* 2021.
- 409 Gao J, Aksoy BA, Dogrusoz U *et al.* Integrative analysis of complex cancer genomics and clinical  
410 profiles using the cBioPortal. *Sci Signal* 2013;**6**:p11.
- 411 Hauschild A, Grob J-J, Demidov LV *et al.* Dabrafenib in BRAF-mutated metastatic melanoma: a  
412 multicentre, open-label, phase 3 randomised controlled trial. *The Lancet* 2012;**380**:358–65.
- 413 Hong DS, Fakih MG, Strickler JH *et al.* KRAS G12C Inhibition with Sotorasib in Advanced Solid  
414 Tumors. *N Engl J Med* 2020;**383**:1207–17.
- 415 Huang JY. The EMOTIF database. *Nucleic Acids Res* 2001;**29**:202–4.
- 416 IEEE, The Open Group. The Open Group Base Specifications Issue 7. 2018.
- 417 Kleene SC. Representation of events in nerve nets and finite automata. *Autom Stud* 1956;**34**:3–41.
- 418 Lynch TJ, Bell DW, Sordella R *et al.* Activating Mutations in the Epidermal Growth Factor Receptor  
419 Underlying Responsiveness of Non-Small-Cell Lung Cancer to Gefitinib. *N Engl J Med*  
420 2004;**350**:2129–39.
- 421 Martincorena I, Campbell PJ. Somatic mutation in cancer and normal cells. *Science* 2015;**349**:1483–9.
- 422 Mersmann O. *Microbenchmark: Accurate Timing Functions.*, 2021.
- 423 Nagurney A. Chapter 7 Parallel computation. Vol 1. Elsevier, 1996, 335–404.

- 424 National Institute of Standards and Technology. *Advanced Encryption Standard (AES)*. Gaithersburg,  
425 MD: National Institute of Standards and Technology, 2001:NIST FIPS 197.
- 426 Ooms J. The jsonlite Package: A Practical and Consistent Mapping Between JSON Data and R Objects.  
427 *ArXiv14032805 StatCO* 2014.
- 428 Paez JG, Jänne P, Lee JC *et al.* EGFR mutations in lung cancer: correlation with clinical response to  
429 gefitinib therapy. *Science* 2004;**304**:1497–500.
- 430 R Core Team. *R: A Language and Environment for Statistical Computing*. Vienna, Austria: R  
431 Foundation for Statistical Computing, 2018.
- 432 Rescorla E. *The Transport Layer Security (TLS) Protocol Version 1.3*. RFC Editor, 2018.
- 433 Tate JG, Bamford S, Jubb HC *et al.* COSMIC: the Catalogue Of Somatic Mutations In Cancer. *Nucleic  
434 Acids Res* 2019;**47**:D941–7.
- 435 The AACR Project GENIE Consortium. AACR Project GENIE: Powering Precision Medicine through  
436 an International Consortium. *Cancer Discov* 2017;**7**:818–31.
- 437 Watson JD, Baker TA, Bell SP *et al.* *Molecular Biology of the Gene*. 6th ed. San Francisco; Cold Spring  
438 Harbor, N.Y.: Pearson/Benjamin Cummings; Cold Spring Harbor Laboratory Press, 2007.
- 439 Yarden Y. The EGFR family and its ligands in human cancer: signalling mechanisms and therapeutic  
440 opportunities. *Eur J Cancer Oxf Engl 1990* 2001;**37 Suppl 4**:S3-8.
- 441 Zhang J, Baran J, Cros A *et al.* International Cancer Genome Consortium Data Portal--a one-stop shop  
442 for cancer genomics data. *Database J Biol Databases Curation* 2011;**2011**:bar026.
- 443 Zheng L-X, Ma S, Chen Z-X *et al.* Ensuring the Correctness of Regular Expressions: A Review. *Int J  
444 Autom Comput* 2021;**18**:521–35.
- 445

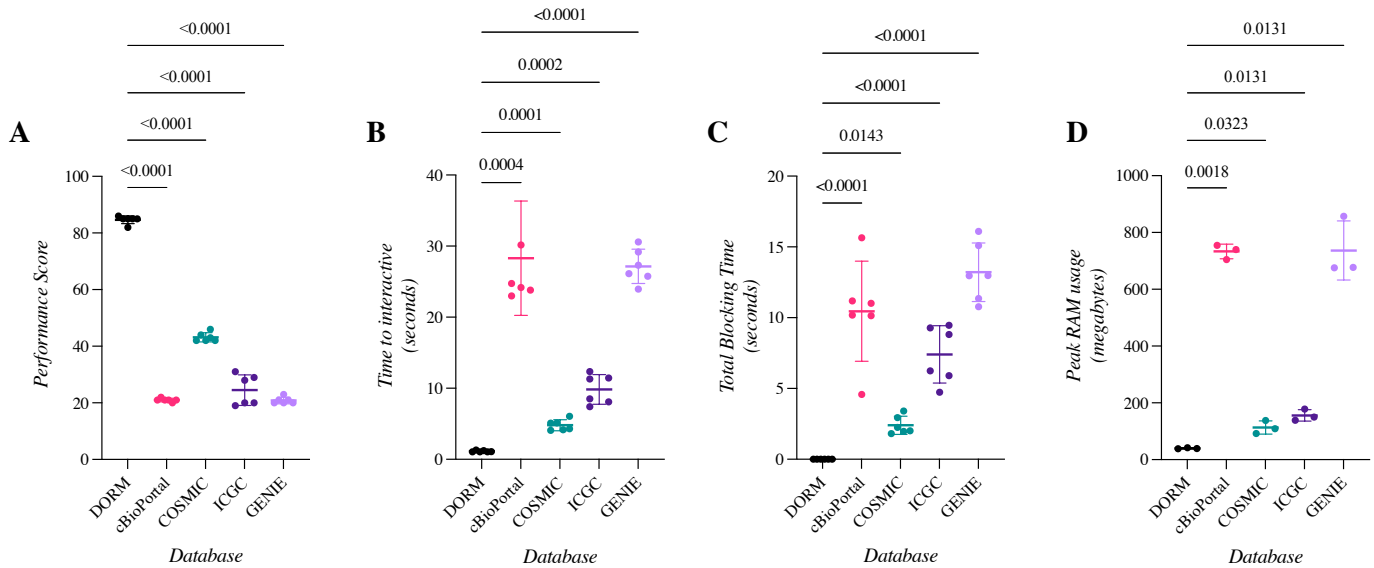


**Figure 1. Comparison of databases and the performance of their websites.**

A search for EGFR mutations was done on each database, and the individual links for that search were used to test the performance of the databases with Google Lighthouse running on Google Chrome web browser. Scatter plots indicating mean and standard deviation of 3 to 6 observations for A) Lighthouse performance score B) Time to interactive (y-axis in seconds) C) Total blocking time (y-axis in seconds) D) Peak memory (RAM) usage by the web pages (y-axis in Megabytes).

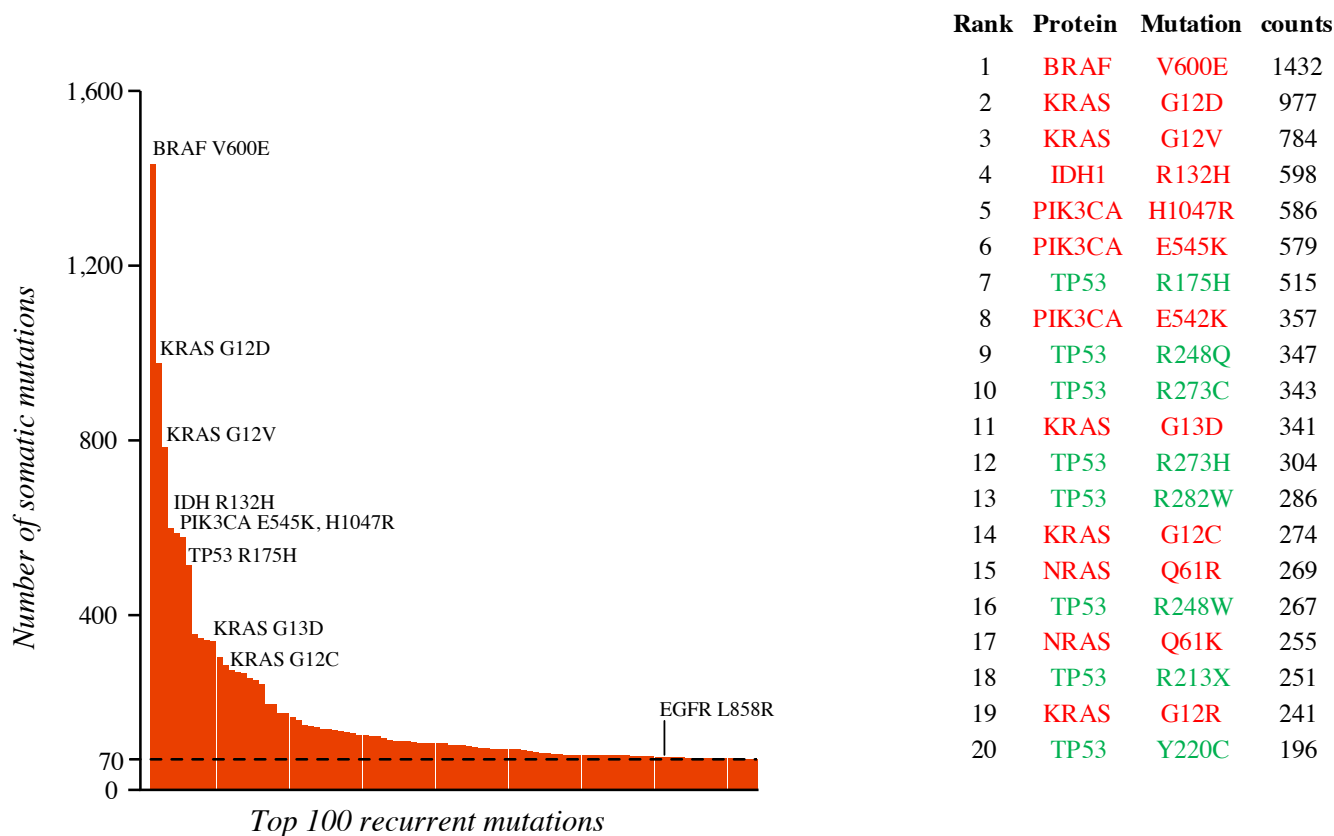


**Figure 2. Distribution of top 100 recurrent mutations.**

Bar plots showing the top 100 most-frequently mutated proteins in the genome-wide somatic mutation data from COSMIC release v95. The top 20 mutations are listed in the table on the right, and the mutations in oncogenes are colored in red and the mutations in tumor suppressors are colored in green.

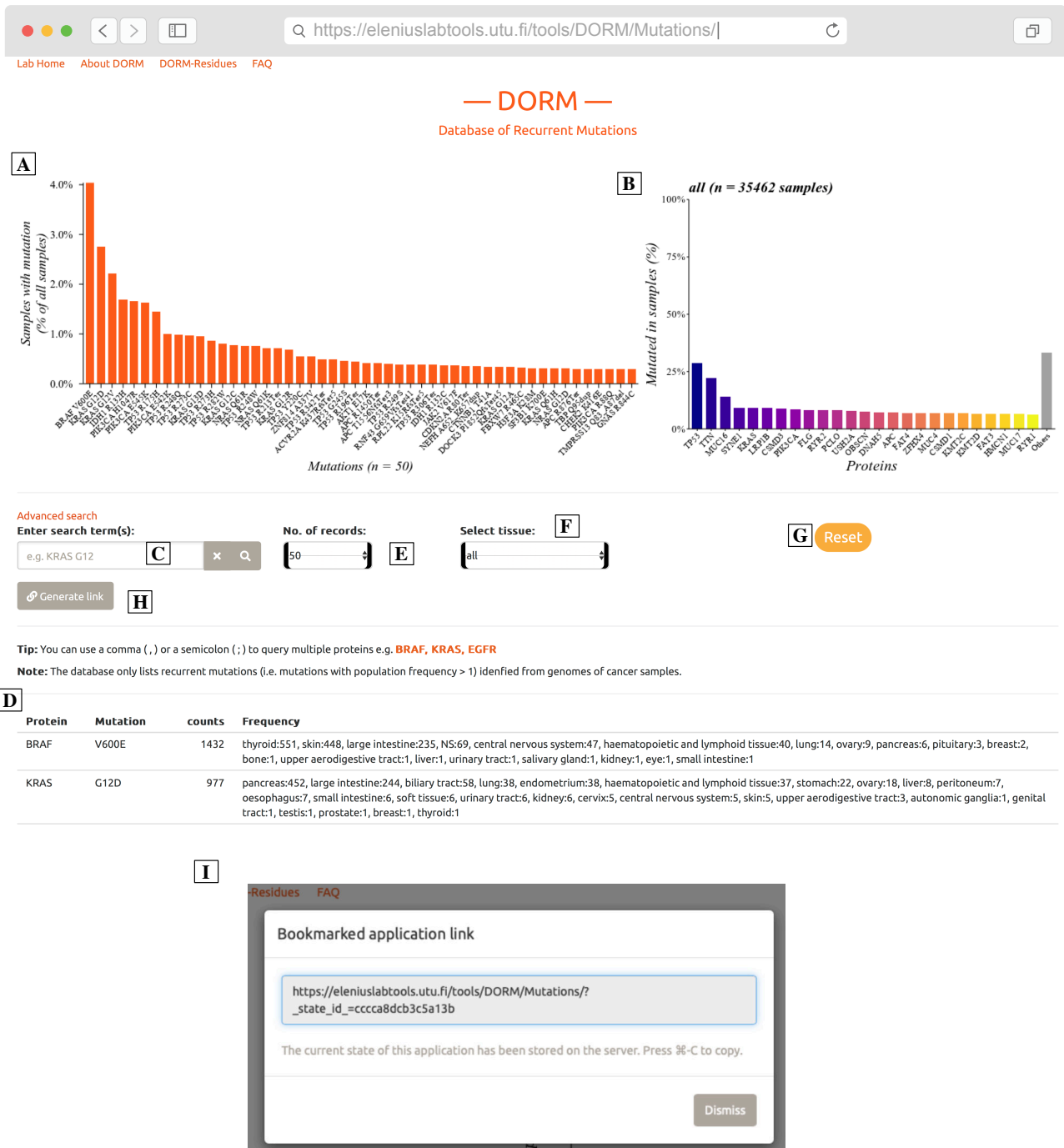


### Figure 3. User interface for DORM : Database Of Recurrent Mutations.

The default GUI of DORM, which hosted at <https://eleniuslabtools.utu.fi/tools/DORM/Mutations/>, shows the information about top 50 most-recurrent mutations identified from genomes of cancer samples. A) Dynamically updated bar plot, responds to search queries, and settings of dropdown menus in "E" and "F". B) A bar chart showing the 25-most frequently mutated genes (color gradient) across all the samples in the selected tissue (can be changed from menu "F"). The "Others" bar represents the percentage of samples not containing mutations in any of the top 25 genes (bars with color gradient). C) The search bar can be used to query the database with several terms, as well as, regular expressions; an example is displayed in gray text. D) Table showing the protein name, mutation (displayed as amino acid change), the number of samples with that exact mutation, and the breakdown of the sample count by primary site of the cancer. E) Dropdown menu can change the number of records displayed in the table "D" and plotted in the bar plot "A". F) Dropdown menu to limit the search to a specific tissue type. G) Button to reset the website and various parameters to their default values. H) Button to generate a direct link to repeat a search with the exact search terms and parameters. Clicking this opens the dialog box "I" which shows the link. I) Dialog box showing the direct link which can be used to conduct the exact search again without having to manually enter search term(s) and set the parameters.

**Fig. 3**

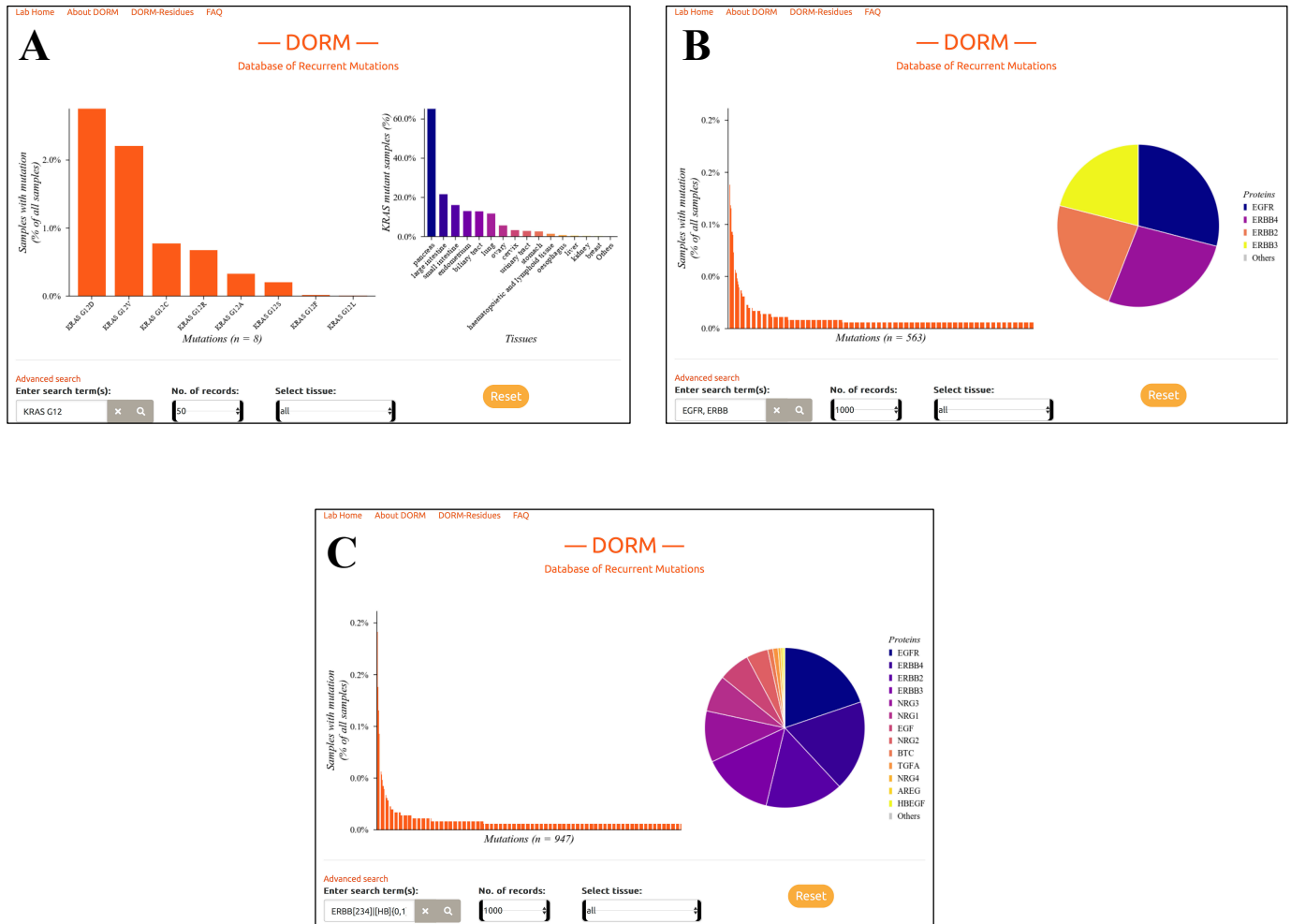


#### Figure 4. Dynamic plots in response to search results.

Based on the context of the search results, DORM automatically generates these specific plots.

A) If the search results (bar plot on the left) consists of just one protein (example results shown here for the query term KRAS G12), the bar plot on the right is updated to show the frequency of mutations in that protein in cancers of various tissues ( $x$ -axis).

B) If the search results contain multiple proteins (query: EGFR, ERBB), a pie chart is displayed with the slices in the pie representing the proportion of mutations that can be attributed to the individual proteins.

C) The distribution of search results when using a regular expression to search the database: ERBB[234]|HB[0,1]EGF[R]{0,1}>|NRG[1-4]|<EP[GR]>|AREG|BTC|TGFA. This regular expression matches the four receptors and eleven ligands in the Epidermal Growth Factor Receptor family of proteins.

**Fig. 4**



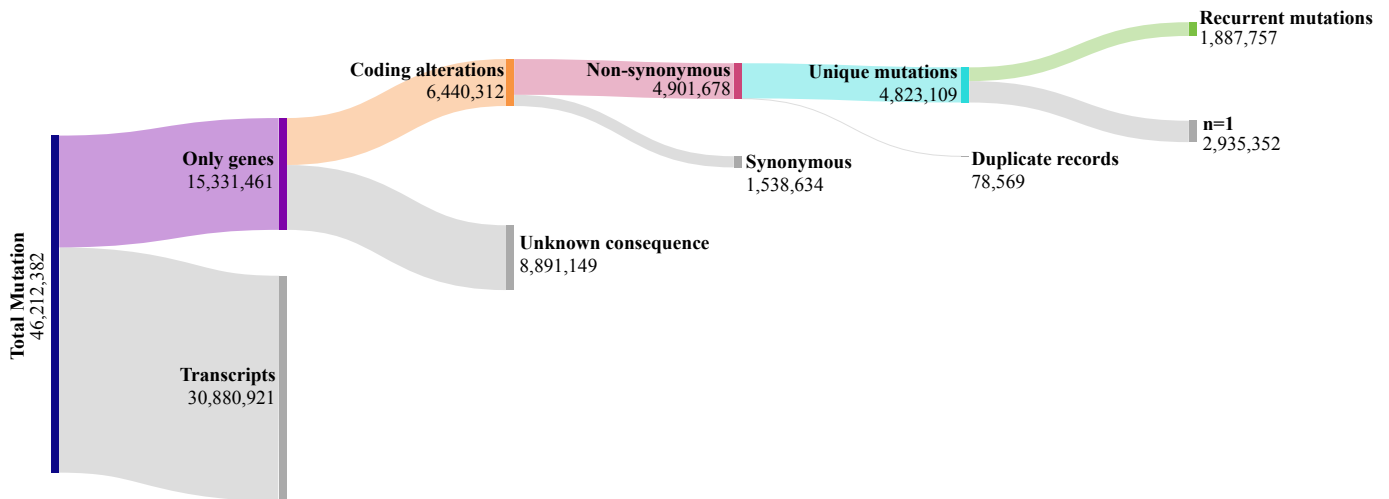


**Figure S1. Filtering scheme to isolate recurrent mutations from COSMIC data.**

Out of 46 million mutations, 30.8 million mutations were removed as they can be attributed to duplicate transcripts of genes. 8.89 million mutations with unreported / unknown consequence were removed. 1.53 million silent mutations were removed, which do not produce any change in the protein. Subsequently, 78,569 duplicate records were removed as they are present due to incorporation of some samples in multiple studies. After this filtering process, 4.82 million unique coding mutations that remained were processed to create the DORM database which summarizes the 1.88 million recurrent mutations (mutations with tissue-agnostic population frequency >1).

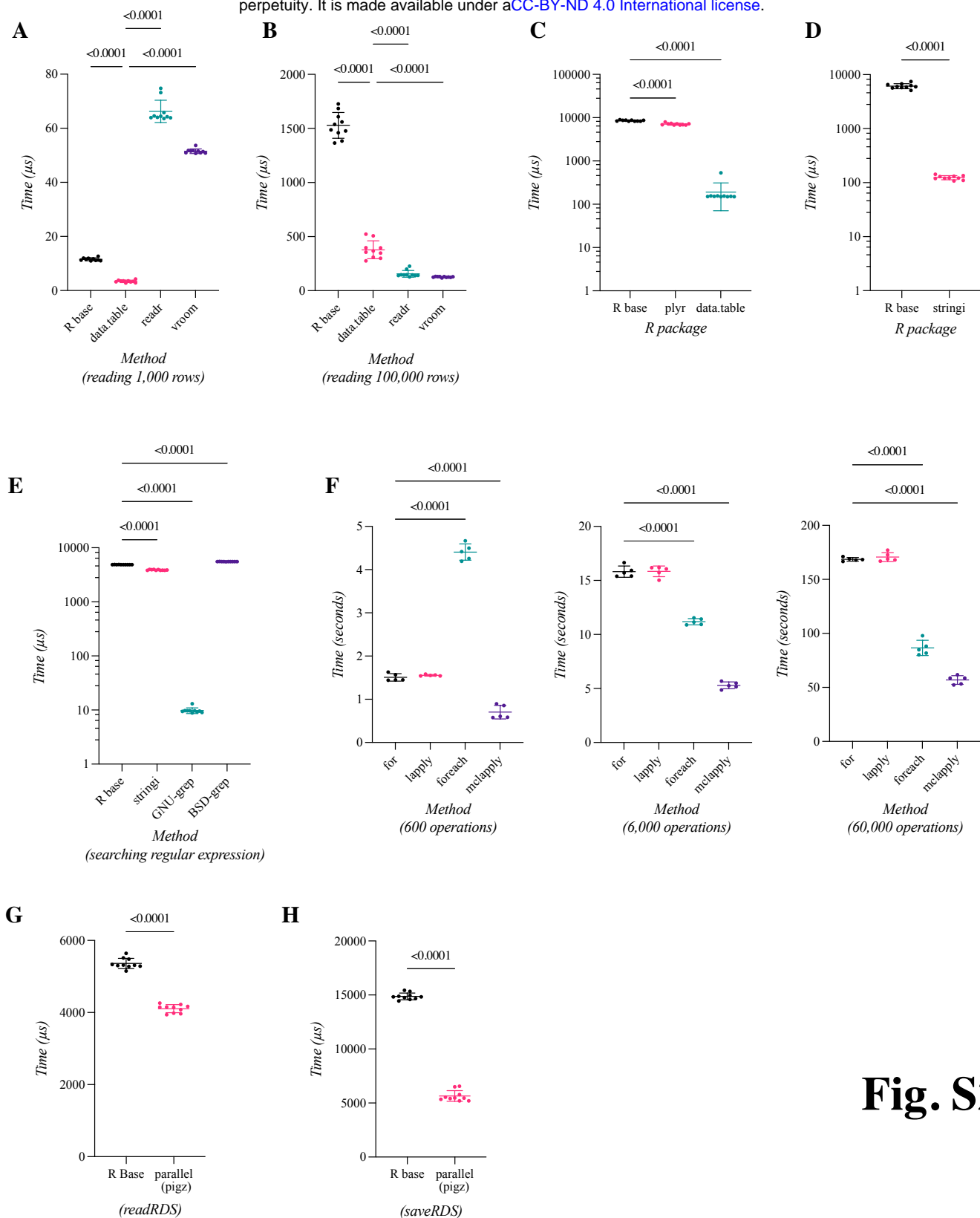


**Fig. S2**

**Figure S2. Comparison of strategies and methods for performing various computational operations.**

Scatter plots showing mean and standard deviation for A-B) Different R packages for reading a tab-separated value (TSV) file or 1000 rows (shown in A) and 100,000 rows (shown in B). C) Various approaches of generating a frequency table. D) Searching for a regular expression (pattern: [ACDEFGHIKLMNPQRSTUVWXYZ]?[0-9]+) using R base and stringi package. E) Searching the data with a regular expression (pattern: EGFR|ERBB[2-4]|[HKN]RAS\>) using the indicated methods. For giving the functions in R the best chance, the data was preloaded in the R outside the code for timing the benchmark. F) Comparing various looping constructs for 600, 6000 and 60000 operations, for and lapply are serialized loops, foreach and mclapply are their parallel alternatives. G) Writing an R object containing a table (1 million rows) as an RDS file with either the R base serialized version or our custom parallelized version using 'pigz' for compression. H) Reading an RDS file (written with our parallel version of saveRDS) with the R base serialized version or our custom parallelized version using 'pigz' for decompression.

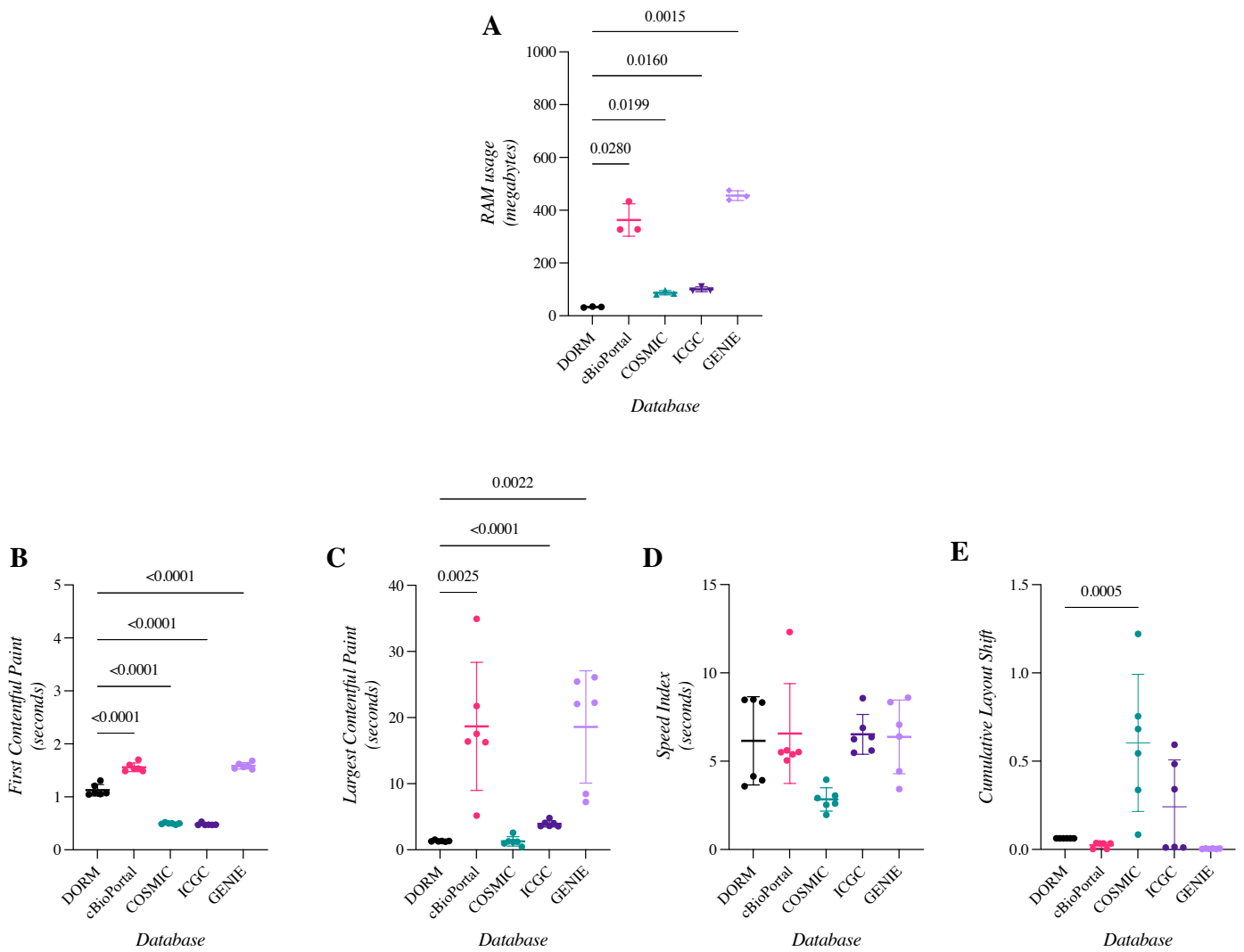


### Figure S3. Comparison of databases and the performance of their websites.

A search for EGFR mutations was done on each database, and the individual links for that search were used to test the performance of the databases with Google Lighthouse running on Google Chrome web browser. Scatter plots with mean and standard deviation for 3 to six observations for A) Memory (RAM) usage after garbage collection (browser idling for 2 minutes) while browsing the indicated databases (y-axis in Megabytes) B) First contentful paint (y-axis in seconds) C) Largest contentful paint (y-axis in seconds) D) Speed index (y-axis in seconds) E) Cumulative layout shift.

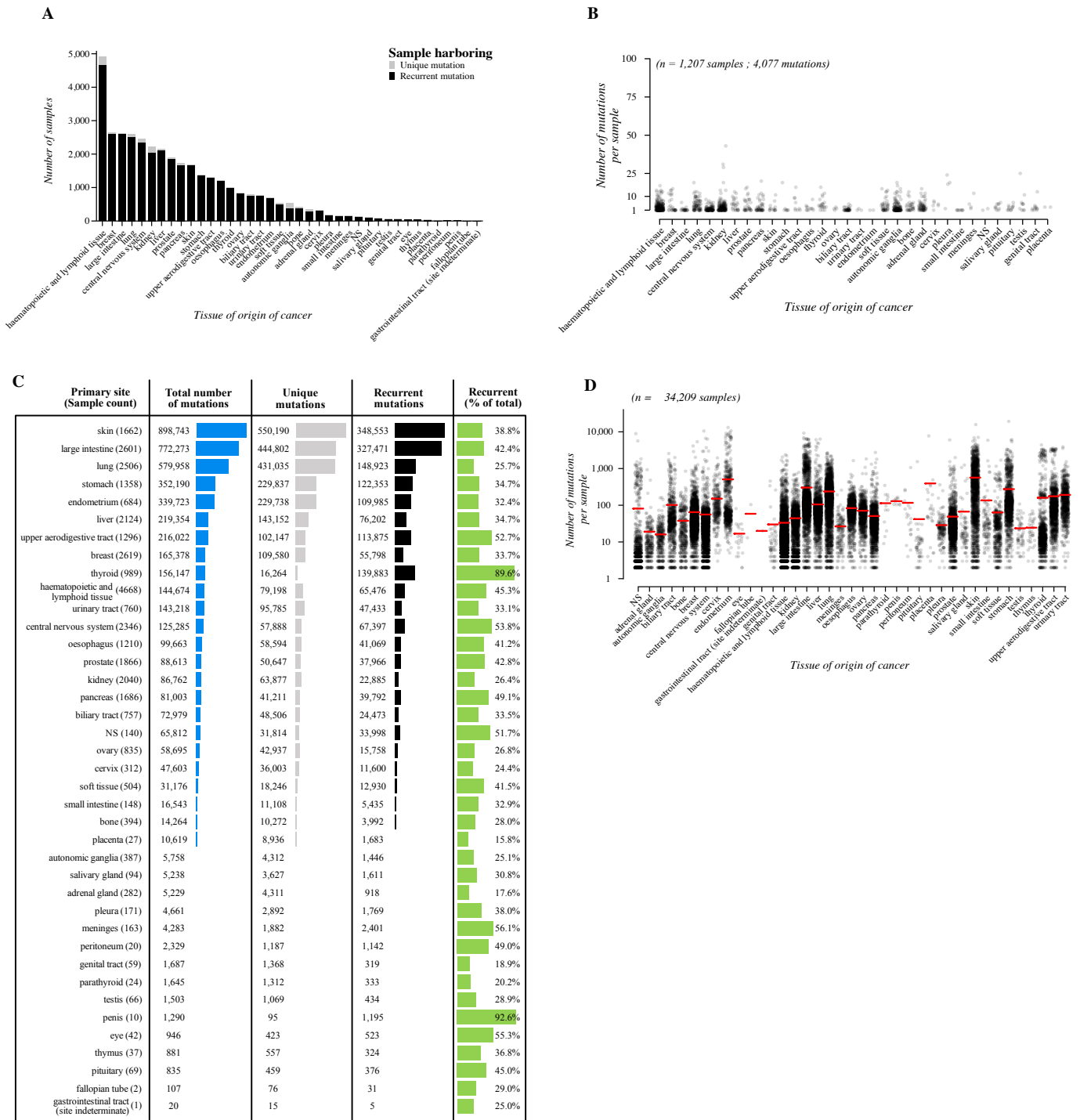


**Figure S4. Distribution of mutations across samples included in the analysis.**

A) Bar chart showing the number of samples harboring at least one recurrent coding mutation, or samples having only unique coding mutations. Recurrent coding mutations are defined as protein sequence-altering mutations with a tissue-agnostic population frequency  $> 1$ . Samples are categorized by primary site of the cancer (x-axis).

B) Dot plot showing the mutational load of individual samples ( $n = 1,207$ ) harboring only unique coding mutations ( $n = 4,077$ ) (i.e., samples comprising the gray part of the bars in panel A). Samples are categorized by primary site of the cancer (x-axis).

C) Distribution of the individual coding mutations categorized by the primary site of the cancer, showing the total number of mutations, the number of unique (mutations never observed in any other sample (tissue-agnostic) in the dataset) and recurrent mutations (tissue-agnostic population frequency  $> 1$ ), and the proportion of the recurrent mutations from the total number of mutations are shown as a percentage.

D) Dot plot showing distribution of mutational load (y-axis in log scale) in samples ( $n = 35,462$ ). Each point represents a sample. Red horizontal line shows the mean mutational load for samples of different primary sites of the cancer (x-axis). NS = tissue is not specified.

| Searching & querying  | DORM     | COSMIC | ICGC  | cBioportal | AACR Genie | Comment   |
|---|----------|--------|-------|------------|------------|---|
| Protein   | Yes      | Yes    | Yes   | Yes        | Yes        |   |
| Individual Mutations (e.g. KRAS G12C)                             | Yes      | Yes    | Yes * | Yes *      | Yes *      | cBioPortal & Genie require searching for the gene and then the mutation. ICGC requires clicking the mutation from a list of results in a dropdown menu. |
| Protein sets  | Yes      | No     | No    | Yes        | Yes        |   |
| Tissues   | Yes      | Yes    | Yes   | No         | No         |   |
| Regular expression  | Yes      | No     | No    | No         | No         |   |
| Substring search (searching for RAS shows HRAS, KRAS, NRAS, etc.) | Yes      | Yes    | Yes   | No         | No         |   |
| <b>Additional features</b>  |          |        |       |            |            | <b>Comment</b>  |
| Direct link to save and share search results                      | Yes      | Yes    | Yes   | Yes        | Yes        |   |
| Summarize by Residue  | Yes      | No     | No    | No         | No         | cBioPortal Lollipop occasionally groups hotspot mutations at a residue as a single lollipop.  |
| Duplicate samples   | No       | Yes    | No    | Yes        | Yes        |   |
| Display most recurrent mutations for a tissue or protein set      | Yes      | No     | Yes   | No         | No         |   |
| Show frequency of a protein being mutated in various tissues      | Yes      | Yes *  | No    | Yes        | No         | Possible on COSMIC Cancer Browser.  |
| Number of rows displayed in table                                 | 10-10000 | 10-100 | 10-50 | 25         | 25         |   |
| Free from cookies, trackers and/or analytics                      | Yes      | No     | No    | No         | No         |   |

**Table 1:** Comparison of features between DORM and other public databases presenting somatic mutations identified from cancer samples. An asterisk indicates a caveat; which is clarified in the corresponding comment column.

| Limitations of DORM                                     | DORM | COSMIC | ICGC | cBioportal | AACR Genie | Comment   |                                    |
|---|------|--------|------|------------|------------|---|------------------------------------|
| Copy number variations & Structural variations          | No   | Yes    | Yes  | Yes        | No         | DORM shows the distribution of mutations in a single protein in different tissues with a pie chart. |                                    |
| Show Lollipop diagram for locating mutations on peptide | No * | No     | Yes  | Yes        | No         |   |                                    |
| Show detailed information (sample and study level)      | No   | Yes    | Yes  | Yes        | Yes        |   |                                    |
| Non coding mutations                                    | No   | Yes    | Yes  | No         | No         |   |                                    |
| Fusions   | No   | Yes    | No   | Yes        | Yes        |   |                                    |
| Select multiple tissues                                 | No   | Yes *  | Yes  | Yes        | No         |   | Possible on COSMIC Cancer Browser. |
| Data download   | No   | Yes    | Yes  | Yes        | No         |   |                                    |

**Table 2:** Limitations of DORM in comparison to other public databases presenting somatic mutations identified from cancer samples. An asterisk indicates a caveat; which is clarified in the corresponding comment column.